Engineering Structures 207 (2020) 110198

Contents lists available at ScienceDirect

Engineering Structures

journal homepage: www.elsevier.com/locate/engstruct

Out-of-plane capacity equations for masonry infill walls accounting for openings and boundary conditions

Laura Liberatore*, Omar AlShawa, Claudia Marson, Monica Pasca, Luigi Sorrentino

Department of Structural and Geotechnical Engineering, Sapienza University of Rome, Via Gramsci 53, 00197 Rome, Italy

ARTICLE INFO

Keywords:
Frame buildings
Experimental data-set
Predictive models
Numerical analysis
Analytical model
Strength prediction
Seismic vulnerability

ABSTRACT

A large part of 20th and 21st centuries' residential buildings is characterised by reinforced concrete, or less frequently steel, frames filled with masonry walls. Recent seismic events have shown that failure of infills may occur under moderate earthquakes, inducing a risk to life and limb of occupants, as well as to construction cost of the building. For this reason, researches have been devoted to the capacity of infill walls carrying out both analytical and experimental tests, also in the out-of-plane direction. These studies have identified the main parameters affecting the out-of-plane response of infill, such as the boundary conditions and the slenderness of the infill.

In this study, a large data set of experimental tests is collected with the aim of investigating the influence of the main factors relevant for the infill response and to assess the suitability of different formulations proposed in the literature. It is found that, for the most part, such formulations underestimate the out-of-plane strength. Afterwards, numerical analyses are performed to investigate those situations that were scarcely considered in experimental campaigns, namely the presence of an opening (window or door) and of a gap between the infill and the top beam. Finally, taking into account all the considered parameters, a formula to predict the out-of-plane strength capacity of an infill is proposed.

1. Introduction

During the last decades, the number of studies focusing on the seismic response of infills has been increasingly growing [1,2]. This is due to the fact that not only does the failure of infills cause life and limb risk and economic losses, but it also affects the global structural response of buildings subjected to earthquake loads. It has been recognised, in fact, that the presence of infills in framed structures modifies their seismic behaviour [3]. The increase of stiffness and strength due the presence of infills leads to a reduction of the deformation demand. An enhancement of the energy dissipation capacity of the system also occurs since masonry dissipates energy through cracking, which occurs at small deformations. Therefore, for moderate intensity of the ground motion, a large part of the energy dissipation is given by the infills, while at higher demand levels, when the infills are severely damaged, the remaining part of the input energy is dissipated by the frame elements [1]. Uniformly distributed infills may prevent the collapse of a building [4,5]. On the other hand, irregular arrangements of infills in plan and/or in elevation, due to poor design or seismic failure, can produce the concentration of high inelastic deformations in some structural elements, leading to a reduction of the global structural capacity [6–8]. Likewise, the presence of strong panels can trigger the failure of lightly shear-reinforced columns [9].

Concerning the in-plane (IP) response of infills, researches date back to the 1950s and include experimental tests, numerical studies and modelling proposals [10–20]. More recently, attention has been devoted also to the out-of-plane (OOP) infill response following the observation that the OOP collapse of infill walls may occur even for moderate intensity of the ground motion [21–24].

Different experimental tests have been carried out to assess the capacity of infills in resisting OOP loading; further details on those experiments will be given and analysed in the paper. Such studies have shown that the main parameters affecting the OOP behaviour are: the slenderness ratio (height/thickness ratio), the aspect ratio (height/length ratio), the masonry compressive strength and, above all, the boundary conditions [25,26]. In addition, the presence of an opening and of prior IP damage were found to affect the OOP response. In the former case the few studies available in the literature up to now present contradictory results.

Numerical methods that recur to one or multiple diagonal struts to

* Corresponding author.
E-mail addresses: laura.liberatore@uniroma1.it (L. Liberatore), omar.alshawa@uniroma1.it (O. AlShawa), claudia.marson@uniroma1.it (C. Marson), monica.pasca@uniroma1.it (M. Pasca), luigi.sorrentino@uniroma1.it (L. Sorrentino).

https://doi.org/10.1016/j.engstruct.2020.110198
Received 1 July 2019; Received in revised form 4 December 2019; Accepted 8 January 2020

model the infills have been proposed to account for the IP/OOP interaction in the investigation of multi-storey buildings (e.g. [27–29]). These approaches are computationally advantageous when static or dynamic analyses of a whole construction are performed.

Alternatively, several analytical models for local verifications have been proposed to predict the OOP strength, like, for example, those based on the one-way arching action [30] or the two-way arching action [31,32]. However, the interaction among different factors is not straightforward and deserves further investigation.

In this study, the OOP response of infill walls is investigated by means of 191 experimental tests available in the literature. The data set includes both reinforced-concrete (RC) and steel frames, as well as confined-masonry structures. The mechanical characteristics of masonry and the boundary conditions between frames and infills of the test specimens take into account a large set of situations, reflecting the great variability in the materials and in the construction techniques adopted in different countries. A number of analytical models are assessed based on the results of such experimental tests. Afterward, numerical analyses are performed to investigate the relative influence of the main factors affecting the OOP capacity and to study those situations not sufficiently investigated so far, namely the presence of an opening (window or door) in the panel and the presence of a top gap. In the analyses, the masonry is modelled by resorting to a smeared-crack approach, while contact surfaces are used at the interface between the masonry panel and the surrounding structure. Geometrical and mechanical characteristics of the panel are varied with the aim of evaluating the influence of different features on the OOP response. Finally, an empirical model is proposed for the evaluation of the OOP strength of infills to be used for local equivalent-static verifications. In the case of existing buildings, this model may help recognise those cases where a strengthening intervention is necessary [33,34].

2. Out-of-plane strength models

Different approaches are available to estimate the OOP strength of masonry infills. Most of them are based on rigid body mechanisms, others are based on numerical or iterative solutions or on the application of finite element (FE) methods. Some analytical models were investigated in Pasca et al. [35]. Additional literature models based on one-way and two-way arching mechanisms are considered hereinafter and compared with a larger experimental database. All these models allow to estimate the strength in a straightforward manner by means of closed form equations (Table 1).

The equation proposed by Angel et al. [36] (see also Abrams et al. [37]) and included in the FEMA 306 recommendations [41], is based on the one-way arching mechanism, originally developed by McDowell et al. [30]. According to this theory, the wall is modelled as an ideal beam supported at the two ends. The masonry material is considered unable to resist tension. Consequently, cracks develop on the tension side at the centre and edges of the wall. After this phase, the two portions are supposed to behave as rigid bodies, rotating around the two edges and the centre (Fig. 1). Further resistance is given by the crushing of the material at hinges location. Formulae derived by Angel et al. [36] based on this theory are then adjusted to match observed experimental results and take into account the effect of IP damage on the OOP resistance by means of the reduction factor R_1 (Eq. (2)) as well as the effect of the frame flexibility by means of the factor R_2 (Eq. (3)).

In Eurocode 6 [38], it is suggested that, in case a wall is built solidly between supports capable of resisting an arch thrust that may develop in horizontal or vertical direction, the analysis may be based on a three-pin arch mechanism according to Eq. (4). Concerning the use of this equation, it is observed that: (i) Eurocode 6 refers to unreinforced masonry walls subjected to lateral loading; (ii) the Eurocode expression can be used when the slenderness ratio does not exceed 20 and the design value of the vertical stress is not less than 0.1 MPa; (iii) for design purposes, the masonry design compressive strength must be used, but hereinafter the experimental strength is considered instead to allow for a more consistent comparison with experimental tests; (iv) in this study, Eq. (4) is included to assess its suitability to infills regardless of the value of the applied vertical stress, which in most experimental tests was less than 0.1 MPa.

Geometric and mechanical parameters considered by models that account for the arching action are also included in the empirical formula proposed by Ricci *et al.* [28] (Eq. (5)), derived from regression analysis on experimental test results. A reduction factor to take into account previous IP damage is also proposed (Eq. (6)) [39].

Equations proposed by Dawe and Seah [31], Flanagan and Bennett [32] and Bashandy et al. [40] are based on the two-way arching action, which develops when the infill is supported along four edges.

Dawe and Seah [31] used virtual work concepts. Specifically, in their approach, the wall is divided into horizontal and vertical strips (Fig. 2); flexural resisting moments between strip segments are then calculated as a function of the compressive strut forces developed by an arching action. A modified yield-line technique is then used to predict post-cracking behaviour and ultimate infill capacity. Based on this procedure, a parametric study to evaluate the effect of several factors on the ultimate load q was performed and Eqs. (7) and (8) proposed for panels supported on four edges and three edges, respectively. The frame flexibility is explicitly considered by means of parameters α (Eq. (9)) and β (Eq. (10)), with $\alpha \leq 50$ for panels supported on four edges, $\alpha \leq 75$ for panels supported on three edges and free at the top and $\beta \leq 50$ in both cases.

Eqs. (7) and (8) were later modified by Flanagan and Bennett [32] based on 36 experimental tests on steel and concrete frames infilled with clay brick and concrete block masonry walls. The numerical constant 4.5 was modified into 4.1 (Eqs. (11) and (12)) and the expressions for parameters α and β were simplified by neglecting the torsional stiffness of the frame members (Eqs. (13) and (14)). In the NZSEE [42] technical guidelines, Eq. (11), multiplied by a reduction factor to account for prior IP cracking, is suggested for the assessment of the OOP infill strength.

In the approach used by Bashandy et al. [40], the panel is divided into vertical and horizontal strip segments experiencing the crack pattern shown in Fig. 2. The maximum OOP deflection is governed by the crushing of masonry in the central vertical strips. The total force resistance Q is calculated assuming an equivalent rectangular stress distribution in the contact area at hinges' location and it is obtained by the sum of the forces resisted by all the vertical and horizontal strips according to Eq. (15), where the first, second and third terms are the forces resisted by the central vertical strips, the lateral vertical strips and the horizontal strips, respectively. Eqs. (16) and (17) give the deflections in the vertical and horizontal directions, respectively, and Eqs. (18) and (19) deliver the resisting moments associated with such deflections.

3. Experimental data

With the aim of investigating the response of infills loaded in the OOP direction and of assessing the reliability of analytical models, experimental results available in the literature are considered hereinafter. The data set, composed of 191 test specimens (Table 2), includes different infill and frame types.

Infills were predominantly made up of solid or hollow clay bricks (159 specimens, combined), whereas concrete blocks were adopted in 32 specimens (Table 3). Mostly, infill walls were not reinforced or strengthened, with the exception of 15 cases, in which masonry was reinforced either with bed-joint or external reinforcements, or strengthened through hybrid glass fiber nets or interior RC grid elements. Just in ten of the experimental tests, a window or door opening was present, therefore a numerical study is performed (see Section 5) to overcome this limitation. Moreover, only four tests were performed on infill cavity walls, while recent experimentation has investigated load-

Table 1
Predictive equations of OOP infill strength.

Reference	Proposed equations	
Angel et al. [36], see also Abrams et al. [37]	$q = \frac{2f_m^{'}}{(h/t)}\lambda R_1 R_2$	(1)
	$R_1 = [1.08 - 0.015(h/t) - 0.00049(h/t)^2 + 0.000013(h/t)^3]^{\frac{\Delta}{2\Delta_{crack}}}$	(2)
	$R_2 = 0.357 + 2.49 \times 10^{-14}$EI when $5.74 \times 10^{12} \leq$ EI $\leq 25.83 \times 10^{12}$ N mm^2	(3)
	$R_2 = 1$ when EI>25.83×10^{12} N mm^2	
Eurocode 6 [38]	$q = f_m^{'}\left(\frac{t}{l_a}\right)^2$	(4)
Ricci et al. [28,39]	$q = 1.95 f_m^{'\,0.35}\frac{t^{1.59}}{h^{2.96}}R_1$	(5)
	$R_1 = \min\{1; 0.14(IDR)^{-1.12}\}$	(6)
Dawe and Seah [31]	panels supported on four edges $q = 4.5(f_m^{'})^{0.75}t^2(\alpha/l^{2.5} + \beta/h^{2.5})$	(7)
	panels supported on three edges $q = 4.5(f_m^{'})^{0.75}t^2\alpha/l^{2.5}$	(8)
	$\alpha = \frac{1}{h}(EI_c h^2 + GJ_c th)^{0.25}$	(9)
	$\beta = \frac{1}{l}(EI_b l^2 + GJ_b tl)^{0.25}$	(10)
Flanagan and Bennett [32]	panels supported on four edges $q = 4.1(f_m^{'})^{0.75}t^2(\alpha/l^{2.5} + \beta/h^{2.5})$	(11)
	panels supported on three edges $q = 4.1(f_m^{'})^{0.75}t^2\alpha/l^{2.5}$	(12)
	$\alpha = \frac{1}{h}(EI_c h^2)^{0.25}$	(13)
	$\beta = \frac{1}{l}(EI_b l^2)^{0.25}$	(14)
Bashandy et al. [40]	$Q = 8\frac{M_{yv}}{h}(l-h) + 8M_{yh}\ln(2) + 8\frac{M_{yh}}{h}\left(\frac{x_{yv}}{x_{yh}}\right)\ln\left(\frac{l}{l-h/2}\right)l$	(15)
	$x_{yv} = \frac{tf_m^{'}}{E_m(1-h/(2\sqrt{(h/2)^2+t^2}))}$	(16)
	$x_{yh} = \frac{tf_m^{'}}{E_m(1-l/(2\sqrt{(l/2)^2+t^2}))}$	(17)
	$M_{yv} = \frac{0.85f_m^{'}}{4}(t-x_{yv})^2$	(18)
	$M_{yh} = \frac{0.85f_m^{'}}{4}(t-x_{yh})^2$	(19)

q = uniform pressure that causes the OOP collapse; $f_m^{'}$ = masonry compressive strength; h = panel height; l = panel length; t = panel thickness; λ = coefficient depending on the slenderness ratio [37]; R_1 = reduction factor accounting for prior IP damage; Δ = IP maximum horizontal displacement; Δ_{crack} = IP displacement at first crack; R_2 = reduction factor that accounts for the flexibility of the confining frame; E = modulus of elasticity of frame material; I = moment of inertia of frame elements; l_a = length or height of the wall between supports capable of resisting an arch thrust; IDR = IP interstorey drift ratio in %; G = shear modulus of frame material, J = torsional constant of frame elements; subscript $_b$ = beams; subscript $_c$ = columns; Q = total OOP force resistance; E_m = modulus of elasticity of masonry. In Eqs. (7), (8), (11) and (12), q and $f_m^{'}$ are expressed in kPa and lengths in mm.

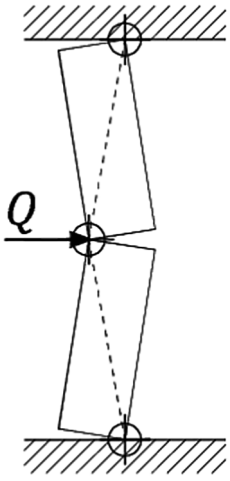

Fig. 1. Schematic representation of the one-way arching mechanism.

bearing cavity walls [43,44]. Due to the lack of a statistically significant database, this infill technique is not specifically investigated hereinafter but, if no wall tie is present, each wythe can be assessed with the equations proposed in the following.

In 83 cases, the frame was made of RC whereas in 33 specimens it was made of steel. Seventy-five walls without frames have been also included if supported at least at two opposite edges of the panel. A summary of frame types is reported in Table 3.

With regard to RC frames, both confined masonries and infilled frames have been considered. They differ to one another for the construction sequence. The confined wall is built before the frame, and the RC is cast against the masonry. Therefore, no gap exists and cohesion develops between the two materials. Moreover, a toothed connection [45] is sometimes prescribed by building codes for the vertical edges, further improving the bond. On the contrary, the infill is built after the frame, therefore a gap may exist especially on the top while at the lateral edges a cohesion is generally present due to the fact that the vertical joints are easily filled with mortar. The effect of a gap between the infill and the top beam was experimentally investigated in few cases (Table 3).

Infills were generally loaded monotonically in the OOP direction by means of airbags or a mid-height beam, while in some cases horizontal forces were applied at the third points or on four points.

Data distribution with varying masonry compressive strength along the vertical direction and slenderness ratio is shown in Fig. 3a and b, respectively. The former varies between 0.5 and 30.5 MPa (Fig. 3a). However, in 63% of cases it is smaller than 6.0 MPa and in 82% of cases it is not greater than 15.0 MPa. Higher values correspond, for the most part, to masonries made of concrete blocks or solid clay bricks. The compressive strength along the horizontal direction can be greater or lower depending on different factors, like for example the presence of

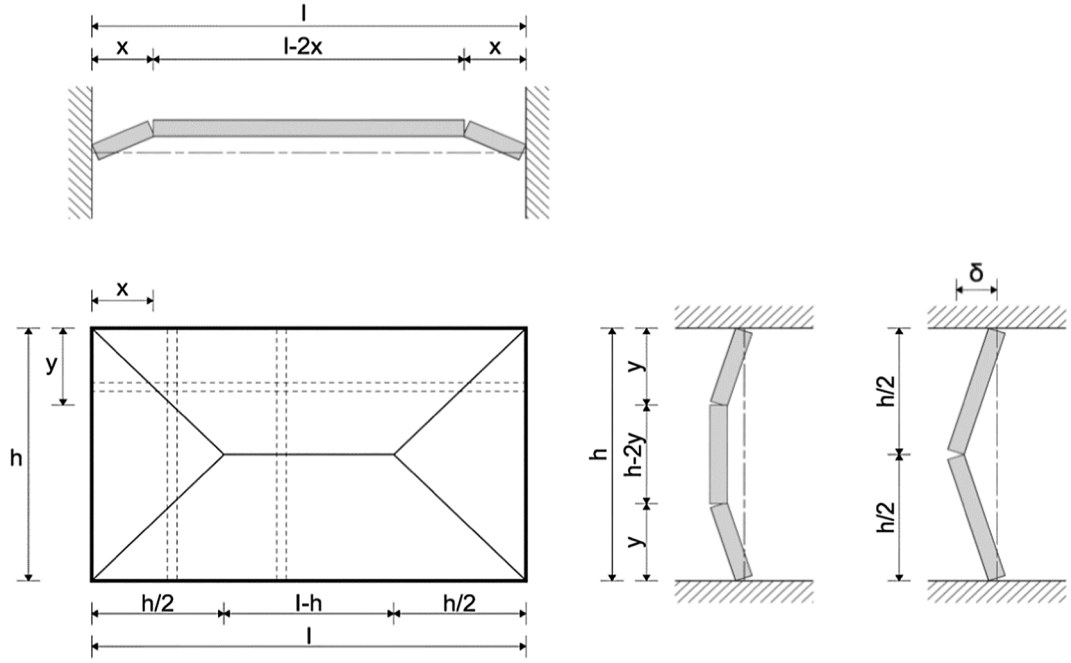

Fig. 2. Crack pattern consistent with a two-way arching mechanism and strip segments.

horizontal or vertical hollows and the type of bond. However, its value is usually not reported in the literature.

The influence of the masonry compressive strength and of the slenderness ratio on the OOP infill experimental resistance is shown in Fig. 4a and b, respectively. The different colors indicate different frame types: blue and yellow markers are adopted for RC and steel frames, respectively, and green markers are used for specimens with no frame. The slenderness effect on the OOP strength is evident, whereas that of the masonry compressive strength is less obvious.

The presence of an opening in the infill was investigated in 10 experimental tests (Table 2). In general, the presence of an opening may prevent the arching effect to fully develop, thus reducing the ultimate resistance. Nonetheless, results of experimental tests indicate that this reduction does not always occur. For example, Dawe and Seah [31] found that the presence of a central opening reduced noticeably the ductility, whereas it did not significantly reduce the capacity. Similarly, the results reported by Griffith et al. [46] show that the presence of a central or eccentric opening did not reduce the OOP strength. Akhoundi et al. [47] observed that the presence of a central opening produced a slight decrease of the initial stiffness and a significant decrease of the

Table 2
Data set of experimental tests.

Reference	No. of test[1]	Frame[2]	Masonry[3]	Boundary conditions[4]	Test type	IP & OOP[5]
Kinstlinger [50]	16	NF	s clay bricks	2 edges	loads at the third points	0
Dawe and Seah [31]	8 (1)	S	vh concrete blocks	3 and 4 edges	airbag	0
Frederiksen [51]	16	ST	s clay bricks	4 edges	airbag	0
Angel et al. [36]	15	RC	s clay bricks, vh concrete blocks	4 edges	airbag	14
Flanagan [52], Flanagan and Bennett [53]	6	S	hh clay bricks	4 edges	airbag	3
Beconcini [54]	33	NF	hh and vh clay bricks	2 edges	load at mid-height	0
Calvi and Bolognini [55]	9	RC	hh clay bricks (6)	4 edges	four points loaded	7
Modena and da Porto [56]	9	NF	hh and vh clay bricks	2 edges	load at mid-height	0
Griffith et al. [46]	8 (6)	NF	vh clay bricks	3 and 4 edges	airbag	0
Komaraneni et al. [57]	3	2 CM, 1 RC	s clay bricks (1)	4 edges	shaking table	3
Varela-Rivera et al. [58]	6	CM	vh concrete blocks	3 and 4 edges	airbag	0
Varela-Rivera et al. [59]	6	CM	vh concrete blocks	4 edges	airbag	0
Pereira et al. [60,61]	8	RC	hh clay bricks (4)	4 edges	airbag	8
da Porto et al. [62]	6	RC	hh and vh clay bricks (4)	4 edges	four points loaded	6
Ingham et al. [63,64]	10	8 NF, 2 CES	s clay bricks	2 and 4 edges	airbag	1
Hak et al. [65]	4	3 RC, 1 NF	vh clay bricks	2 and 4 edges	load at mid-height	3
Furtado et al. [66]	3	RC	hh clay bricks	4 edges	airbag	1
Akhoundi et al. [47]	3 (1)	RC	hh clay bricks	4 edges	airbag	0
Wang [48]	5 (1)	4 RC, 1 S	vh concrete blocks	3 and 4 edges	airbag	1
Sepasdar [49]	4 (1)	RC	vh concrete blocks	4 edges	airbag	1
Ricci et al. [39]	4	RC	hh clay bricks	4 edges	four points loaded	3
De Risi et al. [67]	4	RC	hh clay bricks	4 edges	four points loaded	3
Di Domenico et al. [68]	5	RC	hh clay bricks	2, 3 and 4 edges	four points loaded	0

[1] Total number of tests considered herein, within brackets it is reported the number of specimens with an opening.
[2] RC = Reinforced Concrete, CM = Confined Masonry, S = Steel; ST = Steel Tube, CES = Concrete-Encased Steel, NF = No Frame.
[3] s = solid, vh = vertical hollow, hh = horizontal hollow; within brackets it is reported the number of specimens with reinforced or strengthened masonry.
[4] Number of supported edges.
[5] Number of specimens loaded both IP and OOP.

Table 3
Number of specimens considered in this study.

	No. of specimens
Frame:	
RC	83
Steel	33
No frame[1]	75
Masonry unit:	
Solid clay brick	57
Vertical hollow clay brick	22
Horizontal hollow clay brick	80
Vertical hollow concrete block	32
Boundary conditions:	
Four edges	112
Three edges (top gap)	9
Two edges	70

[1] Panels are supported at least at two opposite edges.

deformation capacity, whereas it did not result in a strength reduction. On the other hand, in the experimental study performed by Wang [48], the presence of a door opening triggered a reduction of the ultimate load of about 45%. Likewise, in Sepasdar [49], the presence of an opening resulted in a 12% decrease of the cracking load and a 34% decrease of the ultimate load. These reductions were also due to the fact that, in both tests, openings were covered with a plywood board, which transferred the pressure to the opening sides, leading to a concentration of damage and, as a consequence, to a decrease of the infill capacity [48].

As for the top gap, it was found that, as expected, it results in a reduction of the OOP strength. The ratio of capacity with a gap to capacity without a gap ranges between 0.28 (in the test carried out by Wang [48]) and 0.95 (in the tests performed by Varela-Rivera et al. [58]).

The interaction between IP and OOP loads was considered in 54 tests, a detailed account of which is reported in Pasca et al. [35]. Generally, prior IP damage reduces the OOP stiffness and strength of the infill. In fact, damage caused by IP forces, e.g. diagonal cracks in the wall or corner crushing, accelerates the OOP collapse. In contrast, prior OOP damage slightly affects the IP strength.

4. Assessment of analytical models

Experimental tests reported in Table 2 are used to assess the capability of the selected analytical formulations (Table 1) to estimate the infill OOP strength. For the comparisons, the whole database is considered. However, with the aim of applying the analytical models properly, for each of them only the experimental tests having characteristics that are taken into account by the model itself are used. For example, concerning the Eurocode 6 [38] equation, which is valid for slenderness ratios not larger than 20, the experimental tests having greater slenderness were disregarded.

The comparison between predicted and experimental values is shown in Fig. 5. Linear regression curves, linear regression ± one logarithmic standard deviation and bisector are also shown in the subplots.

The exponential of the logarithmic mean, $e^{\mu_{ln}}$, and the logarithmic standard deviation, σ_{ln}, of the ratio between predicted and experimental strength are reported in Table 4. The former represents a median value under the hypothesis of a lognormal distribution, the latter, also called dispersion, gives a measure of the variability. Considering the whole database, the formula that, on the average, better predicts the experimental results is that in Eurocode 6 [38], even though it largely overestimates the strength in the case of steel frames. On average, all the models tend to underestimate the strength with some exceptions in the case of steel frames. For steel frames, the model proposed by Bashandy et al. [40] provides adequate predictions, being the exponential of the logarithmic mean equal to 1.18. On the other hand, the logarithmic standard deviation is somewhat high. Generally, the OOP strength of confined masonry is largely underestimated.

Formulae proposed by Dawe and Seah [31] (Eqs. (7), (8)) and Flanagan and Bennett [32] (Eqs. (11), (12)) allow to take into account those cases in which four edges or only three edges are supported by the surrounding frame. This may occur, for instance, when a gap or a weak contact is present between the infill and the top beam. The comparison between experimental results and values estimated by means of the above-mentioned equations highlights that they generally underestimate the strength of infills confined along three edges (Table 5). However, there are several factors that must be taken in consideration when performing such comparisons: (i) in some cases, the conditions of the "3-edges" specimens and their "4-edges" counterparts are slightly different, for example, specimens WE1 and WE2 (see Table 5) have infills with vertical edges mortared to the frame members, whereas in specimens WE6 and WE7, vertical edges are restrained from slipping but not mortared; (ii) Eqs. (7), (8) and (11), (12) were proposed for steel frames whereas most of the experimental tests had a different frame material; (iii) the specimens tested by Griffith et al. [46] had a window opening. In conclusion, not only is the number of experimental

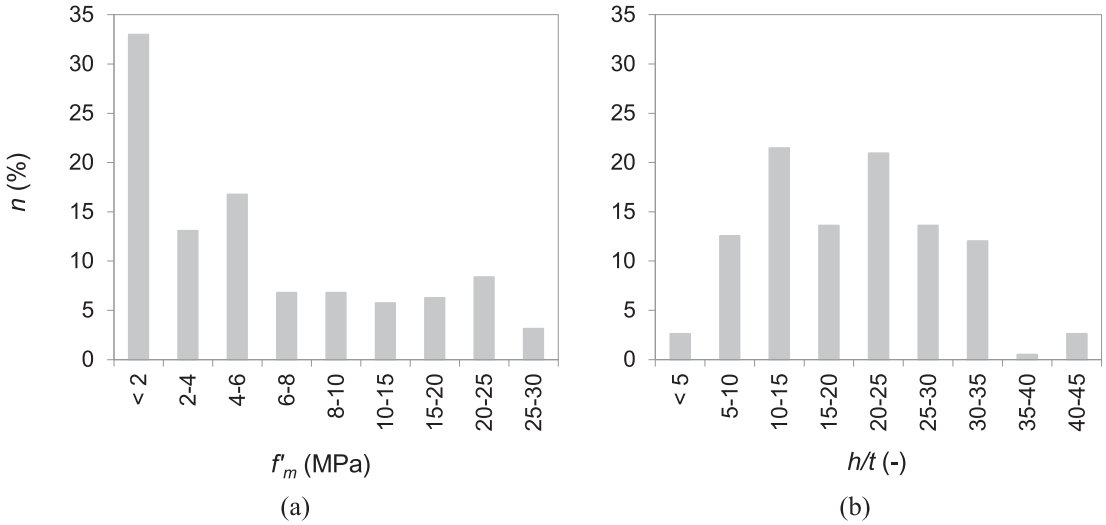

Fig. 3. Data distribution according to: (a) masonry compressive strength along the vertical direction, f'_m, and (b) slenderness ratio, h/t; n in the number of specimens in percentage.

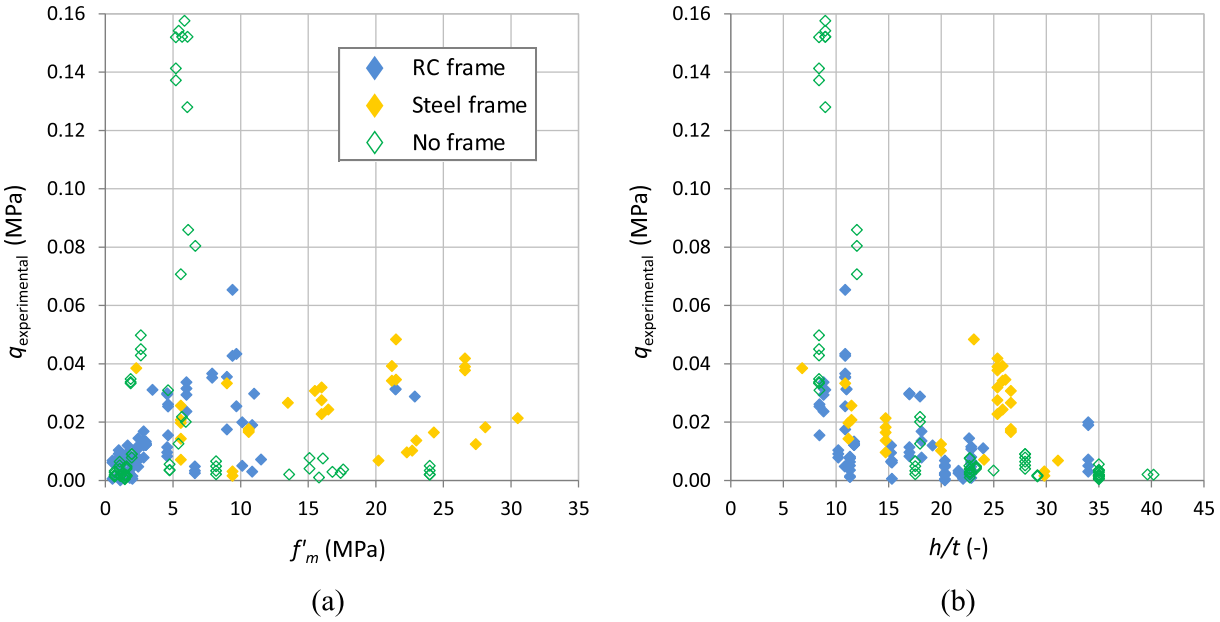

Fig. 4. Experimental OOP infill strength, $q_{experimental}$, versus: (a) masonry compressive strength, f'_m and b) slenderness ratio, h/t.

tests performed on infills supported on three edges low, but it is also somewhat difficult to perform consistent comparisons.

Concerning the prediction of the effect of prior IP damage on the OOP strength, a comparison between experimental results and values predicted by Angel et al. [36] (Eq. (2)) and Ricci et al. [39] (Eq. (6)) is shown in Fig. 6 in terms of the reduction factor, R_{IP}, estimated as the ratio between the OOP strength of specimens previously loaded in the IP direction, q_{IP}, and OOP strength of specimens loaded purely in the OOP direction, q:

$$R_{IP} = \frac{q_{IP}}{q} \tag{20}$$

Clearly, such values are estimated only when a reference specimen, i.e. a specimen tested only with OOP forces, was available. The exponential of the logarithmic mean, $e^{\mu_{ln}}$, and the logarithmic standard deviation, σ_{ln}, which are reported in Fig. 6, indicate that the equation proposed by Angel et al. [36] is adequate, on the average, to predict the IP-OOP interaction, while equation by Ricci et al. [39] is more conservative, underestimating the ratio R_{IP}. It is noted that Eq. (6) [39] is an empirical formula based on experimental results on panels supported along four edges while Eq. (2) [36] although being an analytical model of a one-way arching mechanism, is still calibrated on panels under two-way bending. Therefore, only the reference to different data-set used for their formulations can explain the diverse predictions observed in Fig. 6.

In Fig. 7, experimental R_{IP} values are shown as a function of the interstorey drift ratio (*IDR*). In the same figure, in addition to the Ricci et al. [39] equation, the step-wise formulation suggested by Morandi et al. [69] and the empirical equations proposed by Zizzo et al. [70] are reported. All these formulations provide conservative predictions. On the other hand, they possess the advantageous simplicity of not requiring the displacement at first crack but only the *IDR*, which can be estimated through simplified methods recurring, for instance, to single degree of freedom systems [71].

5. Numerical analysis

5.1. Parametric analysis

A parametric numerical analysis was performed to investigate the influence of the main parameters affecting the OOP response. Slenderness ratio, aspect ratio and masonry strength values are evenly spaced in order to avoid the bias of an overrepresentation of some of them. The presence of an opening in the panel and of a gap between panel and top beam is investigated because experimental data is scarce. Therefore, in the analysis, the presence of a central window or door opening was considered. Furthermore, two boundary conditions were investigated: frame-infill contact on four edges, and on three edges (gap between infill panel and top beam). The following geometrical and mechanical characteristics were considered:

- aspect ratio: h/l = 0.6, 0.75, 1.0;
- slenderness ratio: h/t = 8, 10, 12, 15, 20, 25;
- masonry compressive strength: f'_m = 1.5, 5, 10, 15 MPa;
- central opening: window ($l_o \times h_o$ = 1.2 × 1.0 m^2) or door ($l_o \times h_o$ = 1.0 × 2.0 m^2).

Aspect and slenderness ratios of the infill were varied by changing the infill length and thickness, while the height remained constant and equal to 3 m. Windows and door openings have constant dimensions, which lead to different opening area percentages. Cross sections of frame elements and elastic modulus of concrete are such that the bending stiffness of frame elements, *EI*, is equal to 7.86 × 10^{12} MPa. A summary of models is reported in Fig. 8.

5.2. Modelling

Numerical models were implemented through the LS-DYNA software package [72] within an ANSYS environment. In a previous study, different modelling strategies were investigated and assessed by means of some experimental tests [73]. Among these, the smeared crack approach was found both efficient and able to reproduce the experimental response and was therefore used in the present study. Specifically, masonry infills are modelled as non-linear continua through eight-node solid elements with a single integration point. The major disadvantage of one-point integration is the need to control the zero-energy modes that arise, called “hourglassing” modes, which might enlarge and destroy the solution; to overcome this flaw, a Flanagan-Belytschko stiffness-type stabilisation is used [74]. Contact interfaces, which allow the transmission of both compressive and tensile forces, are employed to model the interaction between masonry and surrounding frame. In compression, to avoid the penetration between nodes of different

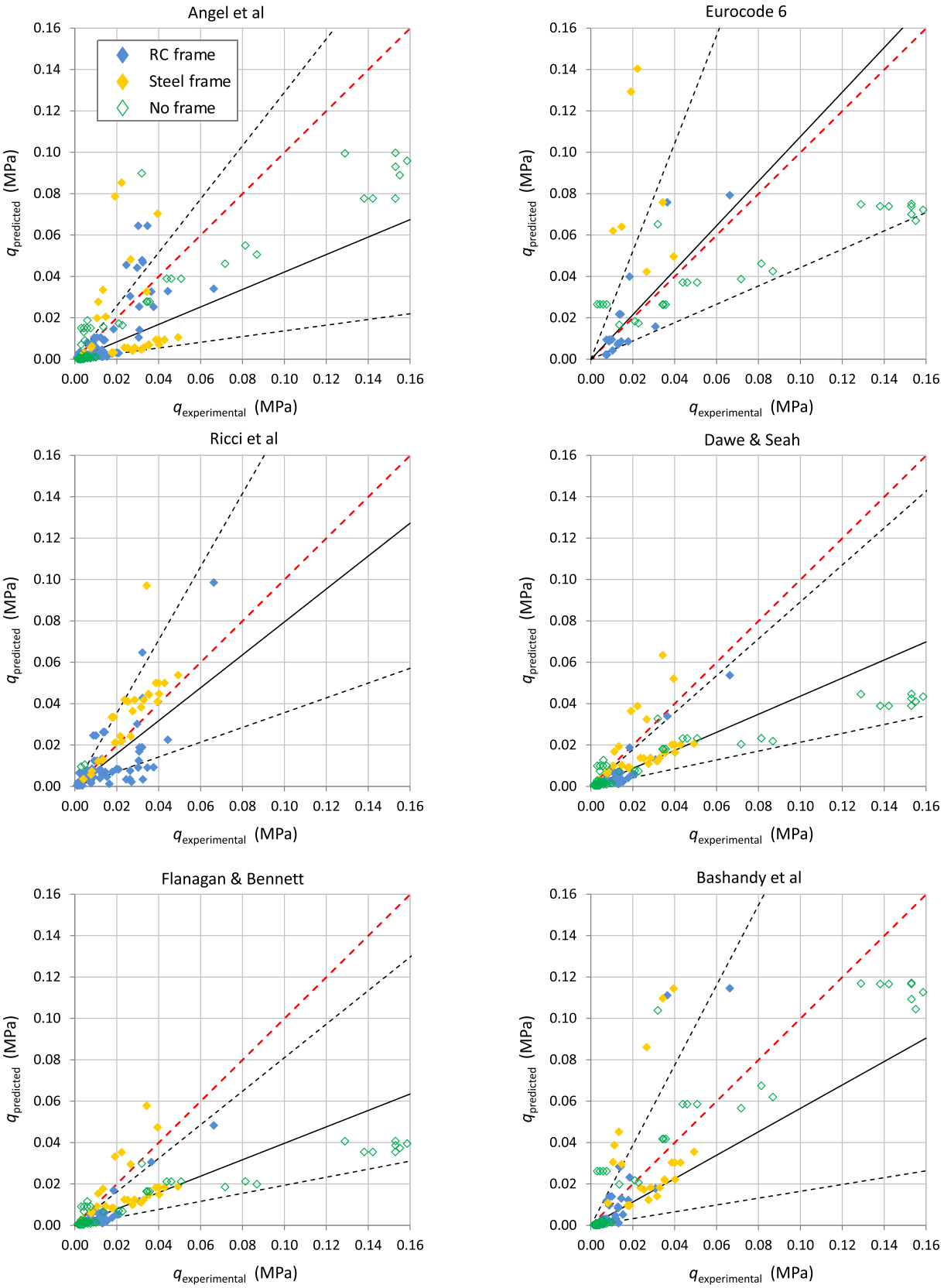

Fig. 5. OOP infill strength (q): predicted vs. experimental values. Solid black line: linear regression; dashed black lines: linear regression ± one logarithmic standard deviation; dashed red line: bisector. Angel *et al.* [36], Eurocode 6 [38], Ricci *et al.* [28,39], Dawe & Seah [31], Flanagan & Bennett [32], Bashandy *et al.* [40]. (For interpretation of the references to colour in this figure legend, the reader is referred to the web version of this article.)

Table 4
Exponential of the logarithmic mean, $e^{\mu_{ln}}$, and logarithmic standard deviation, σ_{ln}, of the ratio between predicted and experimental values of the OOP strength q.

	Angel *et al.* [36]	EC 6 [38]	Ricci *et al.* [28,39]	Dawe & Seah [31]	Flanagan & Bennett [32]	Bashandy *et al.* [40]
Whole database						
$e^{\mu_{ln}}$	0.42	1.08	0.80	0.44	0.40	0.57
σ_{ln}	1.12	0.89	0.80	0.71	0.71	1.23
RC frames						
$e^{\mu_{ln}}$	0.50	0.79	0.63	0.49	0.45	0.62
σ_{ln}	1.02	0.65	0.85	0.69	0.69	1.01
Confined masonries						
$e^{\mu_{ln}}$	0.22	0.94	0.72	0.22	0.20	0.51
σ_{ln}	0.81	0.53	0.78	0.62	0.62	1.20
Steel frames						
$e^{\mu_{ln}}$	0.48	3.36	1.25	0.70	0.64	1.18
σ_{ln}	1.14	0.70	0.29	0.53	0.53	0.92
No frame						
$e^{\mu_{ln}}$	0.38	0.93	–	0.39	0.35	0.40
σ_{ln}	1.25	0.87	–	0.73	0.73	1.31

materials, the standard penalty method is used. The method consists in placing normal springs between surfaces that are in contact. The interface stiffness depends on the stiffness of the materials that are in contact and on the penalty factor. For this parameter, a default value of 0.1 is recommended in the case of contact between similarly refined meshes of comparably stiff materials. However, a value of 0.05, which is more suitable for masonry materials [75,76], is used in this study.

To investigate the influence of specific parameters without introducing further sources of variability, the frame horizontal displacements are not permitted in the OOP direction. At the bottom, the frame is fixed and the masonry panel is connected to a rigid floor by means of contact interfaces.

A linear elastic material is employed for the frame, whereas the Winfrith smeared-crack concrete material model [77] is used for the masonry. The model is defined by initial tangent uniaxial elastic modulus, Poisson's ratio and uniaxial compressive and tensile strengths. As mentioned above, four values of the masonry compressive strength are considered. Tangent modulus and tensile strength are assumed proportional to compressive strength by factors equal to 1000 [38] and 0.1, respectively. Default pressure versus volumetric strain curve is adopted, where the bulk modulus is estimated as a function of the uniaxial tangent modulus and the Poisson's ratio, the latter assumed equal to 0.15. It is observed that the adopted material model does not allow for the modelling of different mechanical characteristics along different directions, for which different modelling strategies should be used.

Gravitational loads are first applied to the model. Static or quasi-static loads are simulated resorting to mass damping to eliminate dynamic oscillations. Moreover, to avoid high frequency oscillations during the application of the gravity loads, these are applied slowly from zero to gravity acceleration. Afterward, horizontal loads are applied monotonically in the OOP direction as body forces, i.e. proportional to the mass. Since the analyses are force-controlled, ultimate displacements and ductility are not evaluated.

5.3. Results and discussion

5.3.1. Solid infills

In Fig. 9, the OOP capacity, in terms of pressure q, is reported as a function of the slenderness ratio for different aspect ratios and masonry compressive strength values. Both the slenderness of the panel and the masonry strength affect noticeably the OOP resistance. Moreover, a resistance increase is noted for aspect ratios approaching one. This effect may be explained by the development of a two-way arching action, which is more pronounced for square panels. In contrast, when one dimension is significantly larger than the other, the arching action tends to develop along the shorter direction.

As shown in Fig. 9, the OOP capacity decreases with decreasing masonry compressive strength. This reduction is more evident for thicker infills (lower slenderness ratios). However, the strength reduction with varying aspect ratio is slightly affected by the masonry compressive strength and by the infill thickness: the ratio between the resistance estimated for aspect ratios lower than 1 and the resistance obtained for the square infill ($h/l = 1$) is almost constant with the variation of the other two parameters. For h/l ratios equal to 0.60 and 0.75 the resistance is, on average, about 0.58 and 0.72 of that for $h/l = 1.00$, respectively. These values confirm experimental evidence according to which the resistance is almost inversely proportional to the span length.

Observed crack patterns are reported in Fig. 10 for a square infill and for an infill having $h/l = 0.6$. The formation of a horizontal crack is followed by diagonal cracks, as also observed during experimental tests on panels supported on four edges [78], where the initial horizontal crack developed along a bed joint near mid-height of the panel and the collapse occurred when additional cracks formed running approximately 45° from the horizontal cracks to the corners of the panels. In the case of a square panel (Fig. 10a), a vertical crack at midspan is also present, consistently with a two-way arching mechanism.

Based on numerical results and considering the influence of the main parameters affecting the OOP strength, the following prediction equation is proposed:

$$q = 0.26 f_m^{'\,0.9} \left(\frac{h}{l}\right)\left(\frac{h}{t}\right)^{-1.23} \tag{21}$$

In this expression, q and $f_m^{'}$ are expressed in MPa. Eq. (21) is valid for panels bounded along 4 edges, with $h \leq l$, and having a masonry compressive strength, $f_m^{'}$, not larger than 15.0 MPa.

Even though Eq. (21) is obtained by regressions based on numerical

Table 5
Experimental and predicted values of the OOP strength of specimens with a top gap and their counterparts supported on four edges.

Reference	infills supported on three edges (top gap)		infills supported on four edges		q_g/q	
	Spec. ID	Exper. q_g[1] (MPa)	Spec. ID	Exper. q[2] (MPa)	Exp. ratio	Pred. ratio[3]
Dawe and Seah [31]	WE6	0.0106	WE2	0.0192	0.55	0.27
	WE7	0.0147	WE1	0.0223	0.66	0.27
Griffith et al. [46]	6	0.0020	5	0.0036	0.56	0.32
Varela-Rivera et al. [58]	E4, E5, E6	0.0132	E1, E2, E3	0.0139	0.95	0.20
Wang [48], Sepasdar [49]	IF-RC-TG	0.0185	IF-ND	0.0663	0.28	0.35
Ricci et al. [39] and Di Domenico et al. [68]	80_OOP_3Eb	0.0057	80_OOP_4E	0.0068	0.84	0.47
	120_OOP_3E	0.0104	120_OOP_4E	0.0130	0.80	0.38

[1] q_g = OOP strength of infills supported on three edges, a top gap is present between the infill and the beam.
[2] q = OOP strength of infills supported on four edges.
[3] Ratios of values predicted by Eqs. (7) and (8) as well as by Eqs. (11) and (12).

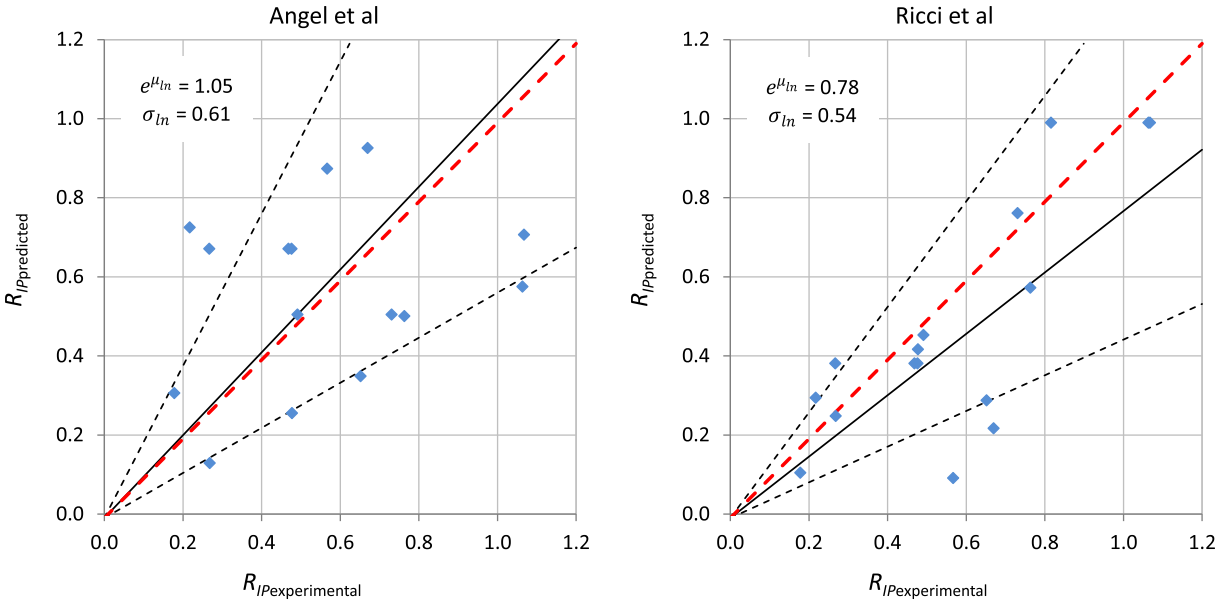

Fig. 6. IP-OOP strength ratio (R_{IP}): predicted vs. experimental values. Solid black line: linear regression; dashed black lines: linear regression ± one logarithmic standard deviation; dashed red line: bisector. Angel *et al.* [36], Ricci *et al.* [28,39]. (For interpretation of the references to colour in this figure legend, the reader is referred to the web version of this article.)

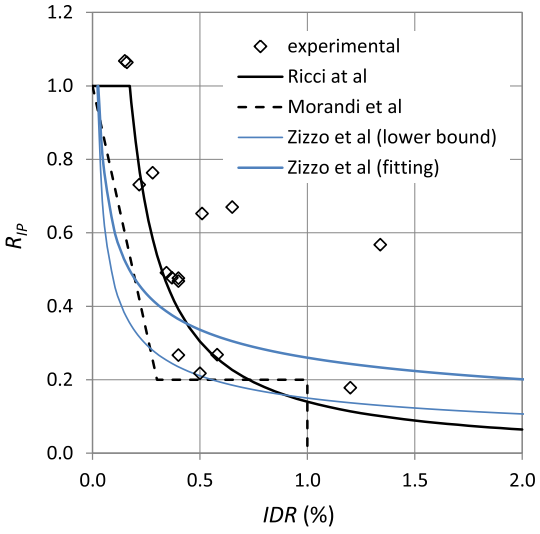

Fig. 7. IP-OOP strength ratio (R_{IP}) vs. interstorey drift ratio *IDR*, experimental values and predictions: Ricci et al. [39], Morandi et al. [69] and Zizzo et al. [70].

analyses, its application to the experimental results described in Section 3 shows that it is particularly suitable for infilled RC frames and confined masonry, i.e. in those situations in which a good contact between infills and surrounding frames exists. In fact, in case of RC frames, the logarithmic mean, $e^{\mu_{ln}}$, and the logarithmic standard deviation, σ_{ln}, of the ratio between predicted and experimental strength are equal to 0.87 and 0.41, respectively, and for confined frames they are equal to 1.07 and 0.25, respectively, markedly better than values in Table 4. On the other hand, the proposed equation overestimates the OOP resistance of infills encased in steel frames, where the infill-frame contact is weaker.

5.3.2. Infills with opening

The presence of a window or door opening modifies the crack pattern on the infills: initial horizontal cracks form close to the top and bottom of the opening, later on, diagonal cracks develop from the opening towards the frame corners (Figs. 11, 12). However, the arching effect may still develop in the masonry portions adjacent to the opening, as also observed by Anić et al. [79]. This phenomenon is more evident in the case of thicker infills, as shown in Fig. 13, where principal stresses are shown along a vertical and a horizontal section.

The presence of an opening leads, in some cases, to an increase of the OOP strength. This apparently contradictory outcome was obtained also by Griffith and Vaculik [80,81]. They explained such result by noting that the total length of diagonal cracks contributing to the wall resistance was mostly unaffected by the presence of an opening and, as a consequence, also the corresponding internal work was unaltered, whereas higher pressure was required to generate the corresponding amount of external work since it acted over a reduced area. In contrast, in some other cases, the presence of an opening produces a reduction of the OOP strength, the amount of which depends on both geometrical and mechanical characteristics of the infill. Obviously, the opening size affects the results, but the dimensions alone are not sufficient to adequately predict the strength reduction. In fact, greater reductions occur in rectangular infills, with higher masonry compressive strength and larger thickness, which means that weaker masonries are less influenced by the presence of an opening. Considering the influence of the above mentioned parameters, the strength reduction due to the presence of an opening can be expressed as:

$$R_o = \frac{q_o}{q} = \min\{1;\ 0.64 - 0.124\ln p_o\} \tag{22}$$

where

$$p_o = \frac{A_o}{A}\frac{l}{h}\frac{t}{h}f_m' \tag{23}$$

R_o is the strength reduction factor, q_o is the OOP resistance of the infill with opening, A_o and A are the opening area and the bay area, respectively. In Eq. (23), f_m' is expressed in MPa.

Eq. (22) is obtained by regressions based on values estimated from numerical analyses; the logarithmic mean, $e^{\mu_{ln}}$, and the logarithmic standard deviation, σ_{ln}, of the ratio between predicted and numerical values of the reduction factor are equal to 1.00 and 0.10, respectively. The reduction factor R_o is depicted in Fig. 14, where numerical and experimental values are also shown. Concerning these latter values, it is worth mentioning that: (i) Fig. 14 shows only those tests in which the infill with an opening had a solid counterpart with reasonably similar

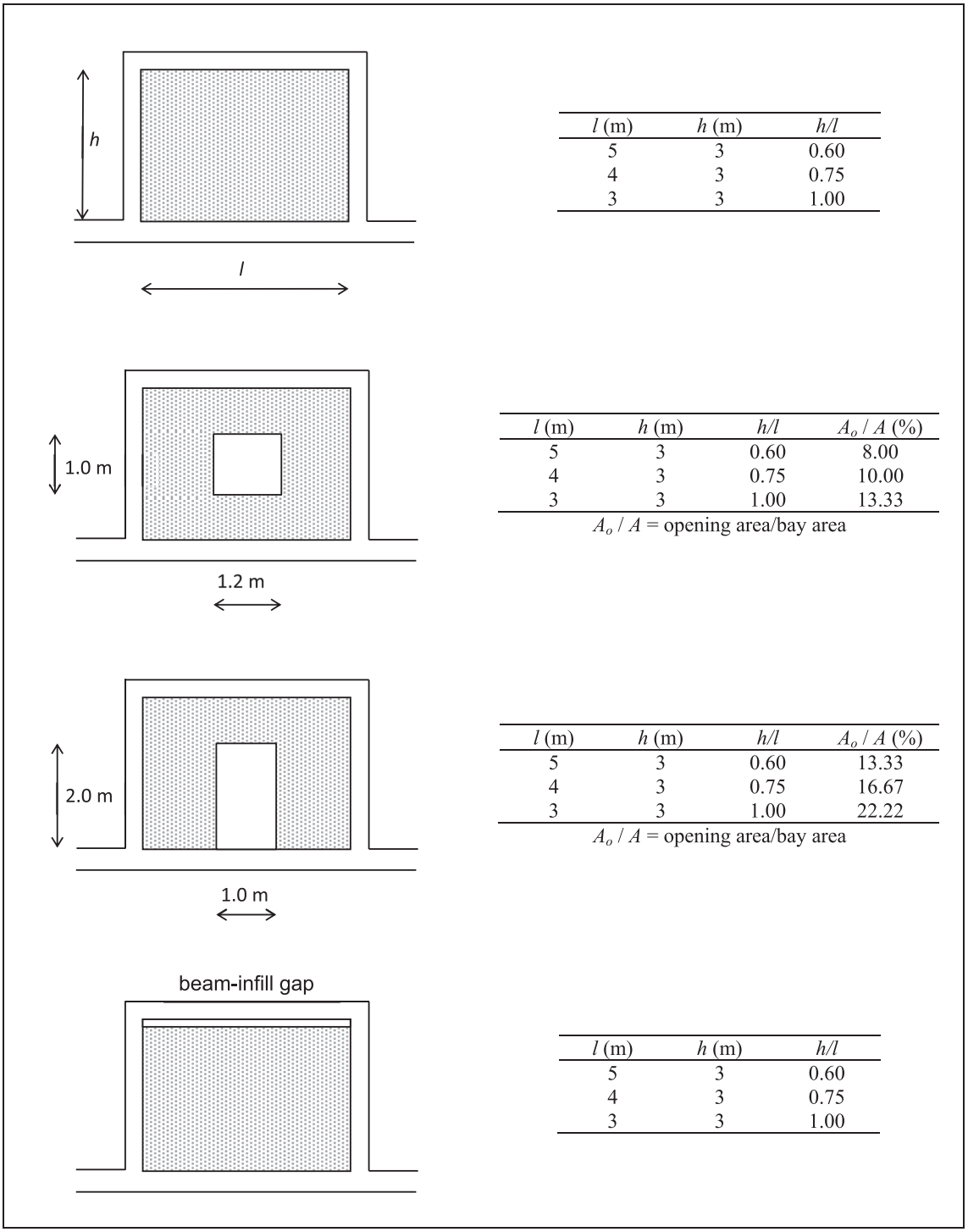

l (m)	h (m)	h/l
5	3	0.60
4	3	0.75
3	3	1.00

l (m)	h (m)	h/l	A_o / A (%)
5	3	0.60	8.00
4	3	0.75	10.00
3	3	1.00	13.33

A_o / A = opening area/bay area

l (m)	h (m)	h/l	A_o / A (%)
5	3	0.60	13.33
4	3	0.75	16.67
3	3	1.00	22.22

A_o / A = opening area/bay area

l (m)	h (m)	h/l
5	3	0.60
4	3	0.75
3	3	1.00

Fig. 8. Geometrical characteristics of the models. For each model, thickness and masonry strength were varied: t = 0.375, 0.30, 0.24, 0.20, 0.15, 0.12 m (h/t = 8, 10, 12, 15, 20, 25); $f_m^{'}$ = 1.5, 5, 10, 15 MPa.

characteristics; (ii) two values are reported for Akhoundi et al. [47] because, even though one infill with opening was tested, two reference frames, built by different workmen, were examined; (iii) in the tests performed by Dawe and Seah [31], the infill with an opening had different interface conditions from those of two reference solid infills; (iv) in most cases, the masonry compressive strength of the infills with the opening was different from that of the infill without opening due to the typical variability of this parameter. However, the logarithmic mean, $e^{\mu_{ln}}$, and the logarithmic standard deviation, σ_{ln}, of the ratio between predicted and experimental reduction factors, R_o, are equal to 0.94 and 0.16, respectively, indicating that Eq. (22) provides a reasonable estimate of such factor.

5.3.3. Infills with gap

A gap between infill and top beam has a noticeable effect on the OOP response. Stress and crack patterns do not change for different geometrical characteristics: a vertical crack originates approximately at midspan. Later on, diagonal cracks develop towards the bottom corners, as shown in Fig. 15 for a square and a rectangular infill. This response is similar to those obtained in experimental campaigns and shows that

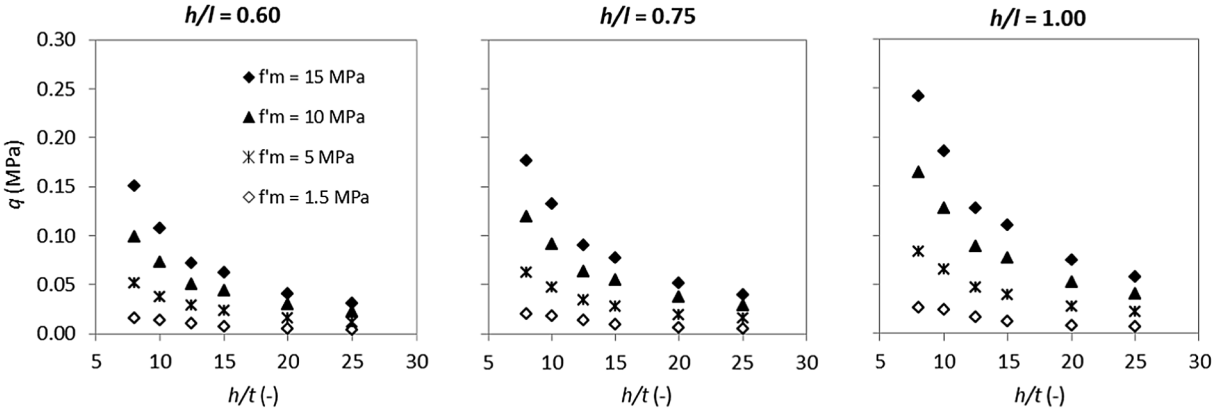

Fig. 9. OOP infill strength, q, estimated from numerical analyses.

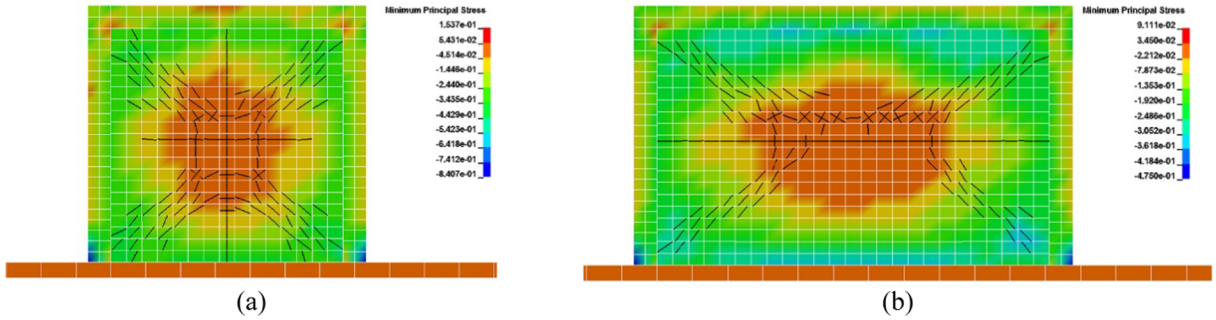

Fig. 10. Crack patterns and 3rd principal stress ($h/t = 10$, $f_m^{'} = 1.5$ MPa): a) $h/l = 1.0$; b) $h/l = 0.6$. Stress in MPa.

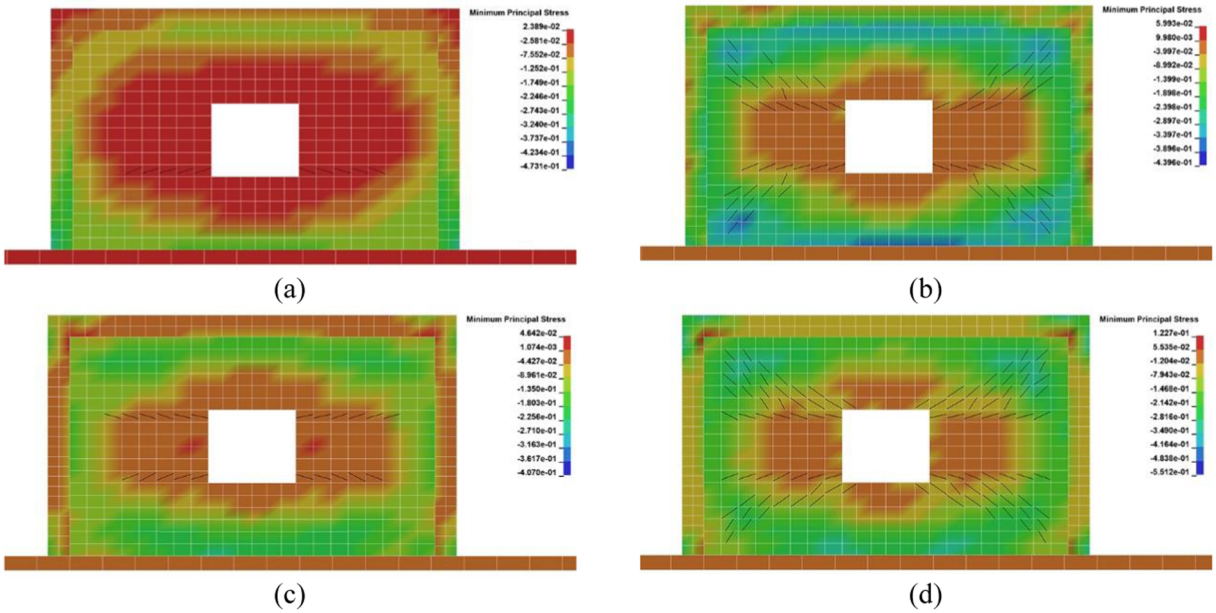

Fig. 11. Crack patterns and 3rd principal stress in infills with a window opening ($h/l = 0.6$, $f_m^{'} = 1.5$ MPa): (a) and (b) $h/t = 10$; (c) and (d) $h/t = 25$; (a) and (c): first crack; (b) and (d): finale stage. Stress in MPa.

one-way arching effect along the horizontal direction may effectively develop. Nonetheless, when a gap is present, the OOP resistance is significantly lower than that of an infill supported on four edges. Numerical analyses performed in this study show that the ratio between the strength of the infill with and without gap does not follow a clear trend with the variables considered and can be expressed by a constant average value:

$$R_g = \frac{q_g}{q} = 0.48 \tag{24}$$

where R_g is the strength reduction factor, i.e. the ratio between the strength of the infill with (q_g) and without (q) a gap. The dispersion, given by the logarithmic standard deviation, σ_{ln}, is equal to 0.14.

Looking at experimental values in Table 5, Eq. (24) tends to be

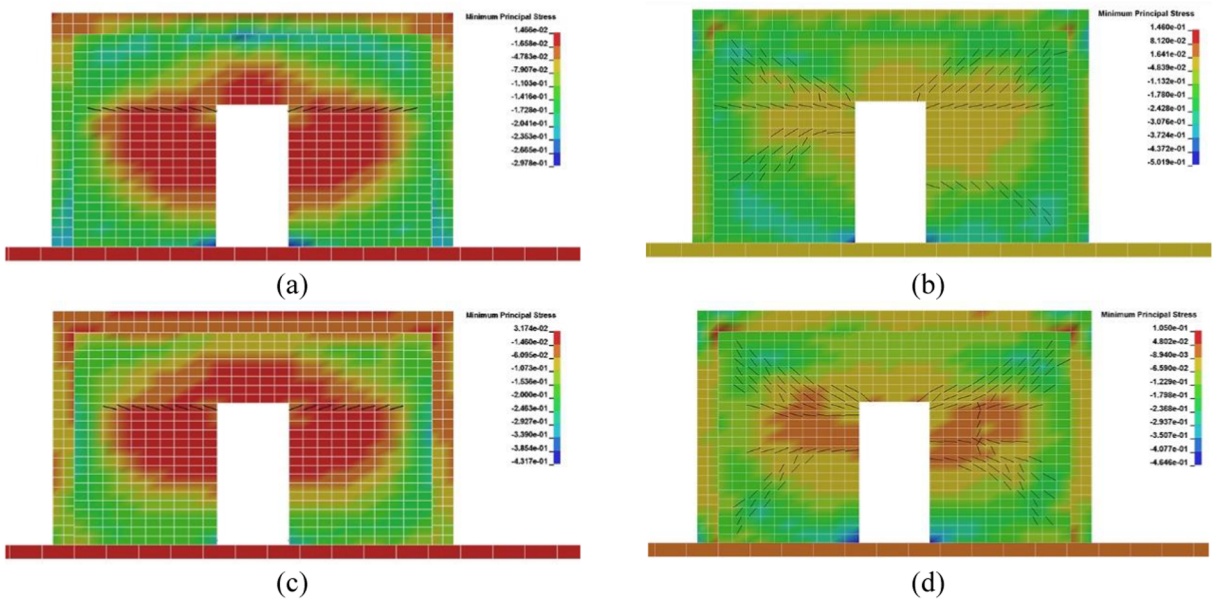

Fig. 12. Crack patterns and 3rd principal stress in infills with a door opening ($h/l = 0.6$, $f_m^{'} = 1.5$ MPa): (a) and (b) $h/t = 10$; c) and d) $h/t = 25$; a) and c): first crack; b) and d): finale stage. Stress in MPa.

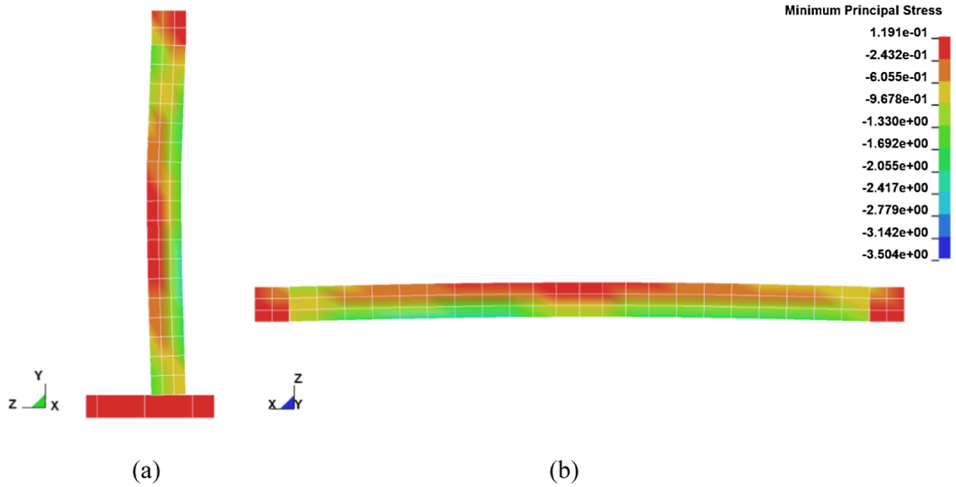

Fig. 13. Deflection and 3rd principal stress for an infill with a window opening ($h/l = 0.6$, $h/t = 10$, $f_m^{'} = 15$ MPa): (a) vertical section; (b) horizontal section. Displacements are not to scale. Stress in MPa.

conservative. Finally, it is worth mentioning that the validity of the above equation is limited to cases in which the gap is at the top of the wall, whereas gaps alongside the columns are not investigated in this study.

5.3.4. Additional remarks

This section deals with some aspects related to the frame and masonry flexibility. As already mentioned, based on Eurocode 6 [38], the tangent modulus of masonry is assumed proportional to its compressive strength by a factor of 1000. The adopted coefficient of proportionality is large compared to what prescribed by other standards for masonry. Therefore, the numerical analyses of the solidly infilled frame with intermediate aspect ratio ($h/l = 0.75$) were repeated assuming $E_m = 700 f_m^{'}$. Results show that, as far as the OOP capacity is concerned, differences are negligible.

To investigate the influence of the frame flexibility, the same analyses were also repeated considering two more values of the bending stiffness of frame elements, namely $EI = 1.86 \times 10^{13}$ MPa (more than twice of the reference value $EI = 7.86 \times 10^{12}$ MPa) and $EI = 1.55 \times 10^{12}$ MPa (about 0.2 of the reference value). It is found that, for the cases under investigation, the increased stiffness does not produce an increase of the OOP capacity of the infill. This indicates that the reference frame is able to sustain the maximum thrust action transmitted by the infill. In contrast, the 80% reduction of the stiffness of columns and beam affects the OOP strength to different extents depending on the masonry compressive strength: for weak masonries ($f_m^{'} = 1.5$ MPa) the effect is negligible, for stronger masonries ($f_m^{'} = 15$ MPa) a decrease between 14% and 19% of the OOP capacity is observed. However, if a concrete elastic modulus of 25×10^3 MPa is considered, the value $EI = 1.55 \times 10^{12}$ MPa corresponds to cross section dimensions of 165×165 mm^2, which are highly unusual in infilled frames and possible, but not common, in confined masonry. In addition, in most situations bounding frame elements are surrounded by neighbouring infilled bays, which hinder their IP deformations [31]. In conclusion, the results obtained herein are valid for $EI \geq 7.86 \times 10^{12}$ MPa or for more flexible frame elements when surrounding infilled bays are present.

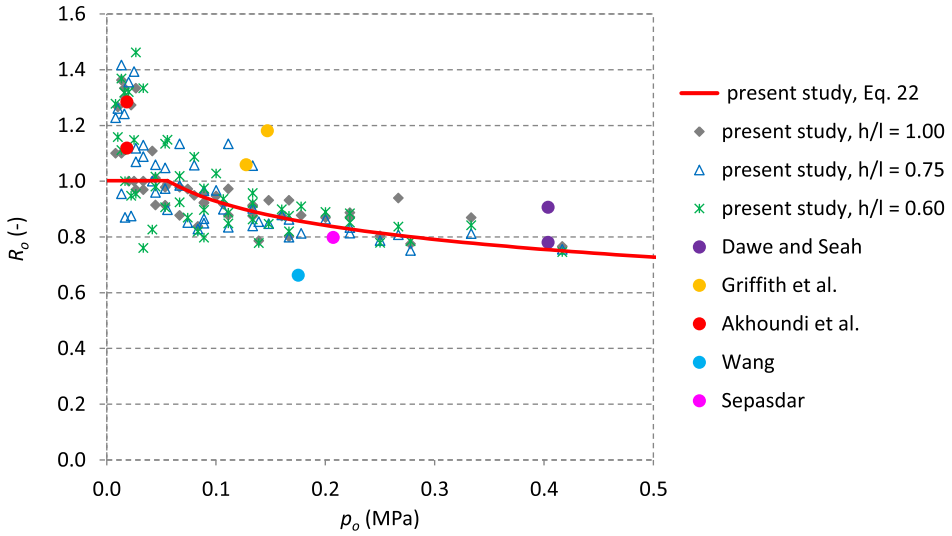

Fig. 14. Opening reduction factor, R_o: comparison between Eq. (22) and values estimated from numerical analyses and experimental tests: Dawe and Seah [31] Griffith et al. [46] Akhoundi et al. [47] Wang [48] Sepasdar [49].

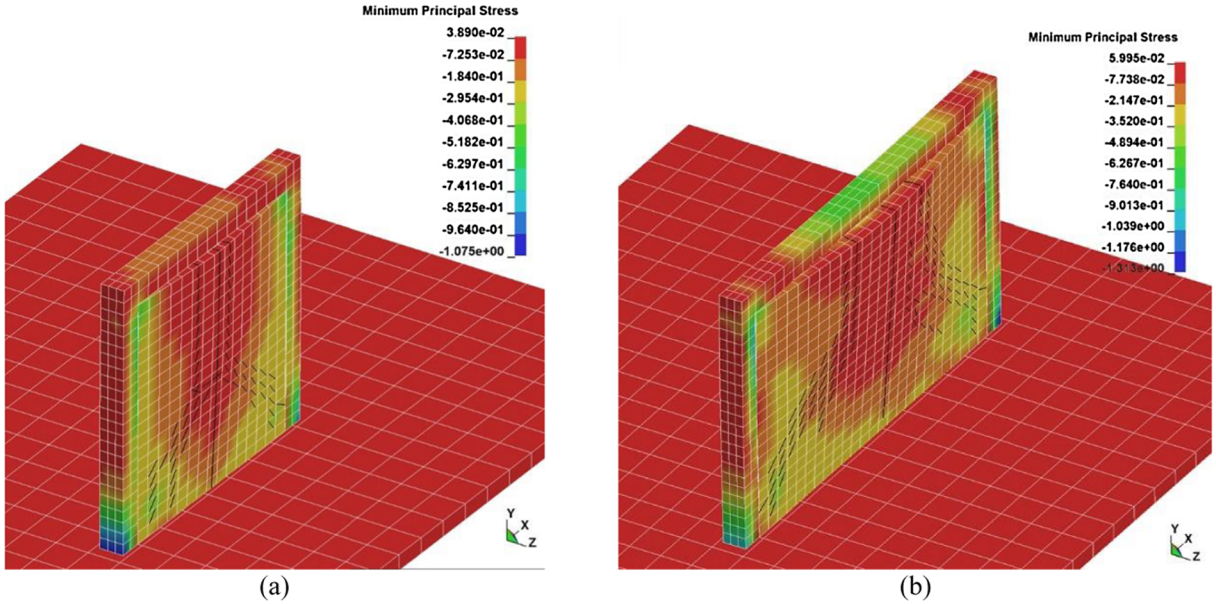

Fig. 15. Deflection, crack pattern and 3rd principal stress for infills with a top gap ($h/t = 10$, $f_m^{'} = 1.5$ MPa): (a) $h/l = 1.0$; (b) $h/l = 0.6$. Displacements are not to scale. Stress in MPa.

6. Conclusions

In this study, the OOP capacity of masonry infills is assessed considering the influence of various parameters. First, a data-set of 191 experimental tests available in the literature is collected, including different types of masonry and frame materials and various boundary conditions. Cases in which the infill was not confined by a frame were also considered, provided that supports were present at least at two opposite edges of the panel.

Experimental results allowed to identify the main parameters affecting the OOP response. Making use of experimental data, different strength prediction equations were also assessed. It can be inferred that most of the models underestimate the capacity of infills encased in RC frames and overestimate that of infills in steel frames. This result may be explained by the different contact conditions between the infill and the surrounding frames, which are generally stronger in case of RC frames, thus leading to a more effective confinement. This aspect deserves further investigation and conclusions of the present work apply to infills encased within RC elements.

A parametric analysis was performed to investigate also those situations that were scarcely considered in experimental campaigns, namely the presence of an opening and of a gap between the infill and the top beam. Four models of RC infilled frames were considered: solid infill, infill with a window opening, infill with a door opening, infill supported on three edges. For each model, aspect ratio, slenderness ratio and masonry compressive strength were varied considering typical values. Based on numerical results, the following equation is proposed to estimate the OOP strength of infill supported on four edges:

$$q = 0.26 f_m^{'\,0.9} \left(\frac{h}{l}\right)\left(\frac{h}{t}\right)^{-1.23} \tag{21}$$

where: q is the uniform pressure that causes the OOP collapse expressed in MPa, $f_m^{'}$ is masonry compressive strength expressed in MPa, h and l are the panel height and length, respectively, and t is panel

thickness; this equation is valid for a panel made up of a masonry with compressive strength up to 15.0 MPa and frame elements having $EI \geq 7.86 \times 10^{12}$ MPa or for more flexible frame elements if surrounding infilled bays are present.

Concerning the presence of an opening, it was found that a reduction of the OOP strength may occur, depending on different parameters, such as the opening dimensions and the masonry compressive strength. A reduction factor, R_o, is suggested to take into account the presence of an opening:

$$R_o = \frac{q_o}{q} = \min\{1;\ 0.64 - 0.124\ln p_o\} \tag{22}$$

where

$$p_o = \frac{A_o}{A}\frac{l}{h}\frac{t}{h}f_m^{'} \tag{23}$$

being q_o the OOP resistance of the infill with opening, A_o and A the opening and the bay area, respectively. In Eq. (23), $f_m^{'}$ is expressed in MPa.

The effect of a gap between the infill and the top beam was also investigated. The results highlighted that the OOP capacity reduces noticeably. In fact, the uniform pressure that causes the OOP collapse when a gap is present can be expressed as $q_g = 0.48q$. All of the above equations were derived by fitting numerical data, therefore if a design value of the masonry compressive strength is adopted in lieu of $f_m^{'}$, they can be conservatively adopted for design purposes.

Finally, if the effect of the IP action on the OOP capacity has to be taken into account, strength reduction factors proposed by Angel et al. [36] and Ricci et al. [39] are suggested, the latter being more conservative.

CRediT authorship contribution statement

Laura Liberatore: Conceptualization, Methodology, Formal analysis, Investigation, Writing - original draft, Supervision, Funding acquisition. **Omar AlShawa:** Methodology, Software, Investigation, Data curation, Validation. **Claudia Marson:** Methodology, Software, Investigation, Data curation. **Monica Pasca:** Conceptualization, Methodology, Writing - review & editing, Visualization. **Luigi Sorrentino:** Conceptualization, Methodology, Resources, Writing - review & editing, Funding acquisition.

Declaration of Competing Interest

The authors declare that they have no known competing financial interests or personal relationships that could have appeared to influence the work reported in this paper.

Acknowledgements

The financial support of the Ministry of the Instruction, University and Research of Italy (MIUR) is gratefully acknowledged. This work has been partially carried out under the program “Dipartimento di Protezione Civile – Consorzio RELUIS”. The opinions expressed in this publication are those of the authors and are not necessarily endorsed by the Dipartimento della Protezione Civile. Three anonymous reviewers are acknowledged for their comments and suggestions.

References

[1] Tarque N, Candido L, Camata G, Spacone E. Masonry infilled frame structures: state-of-the-art review of numerical modelling. Earthq Struct 2015;8:733–59. https://doi.org/10.12989/eas.2015.8.3.733.

[2] Mohammad Noh N, Liberatore L, Mollaioli F, Tesfamariam S. Modelling of masonry infilled RC frames subjected to cyclic loads: state of the art review and modelling with OpenSees. Eng Struct 2017;150:599–621. https://doi.org/10.1016/j.engstruct.2017.07.002.

[3] Asteris PG, Repapis CC, Repapi EV, Cavaleri L. Fundamental period of infilled reinforced concrete frame structures. Struct Infrastruct Eng 2017;13:929–41. https://doi.org/10.1080/15732479.2016.1227341.

[4] Decanini LD, Liberatore L, Mollaioli F. Damage potential of the 2009 L’aquila, Italy, earthquake. J Earthq Tsunami 2012;6. doi:10.1142/S1793431112500327.

[5] De Luca F, Verderame GM, Gómez-Martínez F, Pérez-García A. The structural role played by masonry infills on RC building performances after the 2011 Lorca, Spain, earthquake. Bull Earthq Eng 2014;12:1999–2026. https://doi.org/10.1007/s10518-013-9500-1.

[6] Verderame GM, De Luca F, Ricci P, Manfredi G. Preliminary analysis of a soft-storey mechanism after the 2009 L’Aquila earthquake. Earthq Eng Struct Dyn 2011;40:925–44. https://doi.org/10.1002/eqe.1069.

[7] Liberatore L, Decanini LD. Effect of infills on the seismic response of high-rise RC buildings designed as bare according to Eurocode 8. Ing Sismica 2011;28:7–23.

[8] Tanganelli M, Viti S, de Stefano M, Reinhorn AM. Influence of infill panels on the seismic response of existing RC buildings: a case study. Geotech Geol Earthq Eng 2013;24:119–33. https://doi.org/10.1007/978-94-007-5377-8_9.

[9] Blasi G, De Luca F, Aiello MA. Brittle failure in RC masonry infilled frames: the role of infill overstrength. Eng Struct 2018. https://doi.org/10.1016/j.engstruct.2018.09.079.

[10] Mehrabi AB, Benson Shing P, Schuller MP, Noland JL. Experimental evaluation of masonry-infilled RC frames. J Struct Eng 2002;122:228–37. https://doi.org/10.1061/(asce)0733-9445(1996) 122:3(228).

[11] Dolšek M, Fajfar P. The effect of masonry infills on the seismic response of a four storey reinforced concrete frame-a probabilistic assessment. Eng Struct 2008;30:3186–92. https://doi.org/10.1016/j.engstruct.2008.04.031.

[12] Cavaleri L, Di Trapani F. Cyclic response of masonry infilled RC frames: experimental results and simplified modeling. Soil Dyn Earthq Eng 2014;65:224–42. https://doi.org/10.1016/j.soildyn.2014.06.016.

[13] Decanini LD, Liberatore L, Mollaioli F. Strength and stiffness reduction factors for infilled frames with openings. Earthq Eng Eng Vib 2014;13:437–54. https://doi.org/10.1007/s11803-014-0254-9.

[14] Liberatore L, Mollaioli F. Influence of masonry infill modelling on the seismic response of reinforced concrete frames. Proc Fifteenth Int Conf Civil, Struct Environ Eng Comput 2015. https://doi.org/10.4203/ccp.108.87.

[15] Iervolino I, Baltzopoulos G, Chioccarelli E, Suzuki A. Seismic actions on structures in the near-source region of the 2016 central Italy sequence. Bull Earthq Eng 2017:1–19. doi:10.1007/s10518-017-0295-3.

[16] Chiozzi A, Miranda E. Fragility functions for masonry infill walls with in-plane loading. Earthq Eng Struct Dyn 2017;46:2831–50. https://doi.org/10.1002/eqe.2934.

[17] Morandi P, Hak S, Magenes G. Performance-based interpretation of in-plane cyclic tests on RC frames with strong masonry infills. Eng Struct 2018;156:503–21. https://doi.org/10.1016/j.engstruct.2017.11.058.

[18] Liberatore L, Noto F, Mollaioli F, Franchin P. Comparative assessment of strut models for the modelling of in-plane seismic response of infill walls. In: COMPDYN 2017, 6th Int conf comput methods struct dyn earthq eng; 2017. doi:10.7712/120117.5643.17476.

[19] Asteris PG, Cavaleri L, Di Trapani F, Tsaris AK. Numerical modelling of out-of-plane response of infilled frames: state of the art and future challenges for the equivalent strut macromodels. Eng Struct 2017;132:110–22. https://doi.org/10.1016/j.engstruct.2016.10.012.

[20] Liberatore L, Noto F, Mollaioli F, Franchin P. In-plane response of masonry infill walls: comprehensive experimentally-based equivalent strut model for deterministic and probabilistic analysis. Eng Struct 2018;167:533–48. https://doi.org/10.1016/j.engstruct.2018.04.057.

[21] Braga F, Manfredi V, Masi A, Salvatori A, Vona M. Performance of non-structural elements in RC buildings during the L’Aquila, 2009 earthquake. Bull Earthq Eng 2011;9:307–24. https://doi.org/10.1007/s10518-010-9205-7.

[22] Inel M, Ozmen HB, Akyol E. Observations on the building damages after 19 May 2011 Simav (Turkey) earthquake. Bull Earthq Eng 2013;11:255–83. https://doi.org/10.1007/s10518-012-9414-3.

[23] Masi A, Chiauzzi L, Santarsiero G, Manfredi V, Biondi S, Spacone E, et al. Central Italy earthquake: the Amatrice case study. Bull Earthq Eng 2016;2017:1–24. https://doi.org/10.1007/s10518-017-0277-5.

[24] Perrone D, Calvi PM, Nascimbene R, Fischer EC, Magliulo G. Seismic performance of non-structural elements during the 2016 Central Italy earthquake. Bull Earthq Eng; 2018. p. 1–23. doi:10.1007/s10518-018-0361-5.

[25] Liberatore L, Pasca M. Assessment of the out-of-plane resistance of masonry infill walls. In: Proc fifteenth int conf civil, struct environ eng comput; 2015. doi:10.4203/ccp.108.173.

[26] Liberatore L, Marson C, AlShawa O, Pasca M, Sorrentino L. Failure of masonry infill walls under out-of-plane loads. Proc Int Mason Soc Conf 2018:78–88.

[27] Mosalam KM, Günay S. Progressive collapse analysis of reinforced concrete frames with unreinforced masonry infill walls considering in-plane/out-of-plane interaction. Earthq Spectra 2015;31:921–43. https://doi.org/10.1193/062113EQS165M.

[28] Ricci P, Di Domenico M, Verderame GM. Empirical - based out - of - plane URM infill wall model accounting for the interaction with in - plane demand. Earthq Eng Struct Dyn 2018;47:802–27. https://doi.org/10.1002/eqe.2992.

[29] Di Trapani F, Shing PB, Cavaleri L. Macroelement model for in-plane and out-of-plane responses of masonry infills in frame structures. J Struct Eng (United States) 2018;144. https://doi.org/10.1061/(ASCE)ST.1943-541X.0001926.

[30] McDowell EL, McKee KE, Sevin E. Arching theory of masonry walls. J Struct Div 1956;82. 915–1–915–8.

[31] Dawe JL, Seah CK. Out-of-plane resistance of concrete masonry infilled panels. Can J Civ Eng 1989;16:854–64. https://doi.org/10.1139/l89-128.

[32] Flanagan RD, Bennett RM. Arching of masonry infilled frames: comparison of analytical methods. Pract Period Struct Des Constr 1999;4:105–10.
[33] Walsh KQ, Dizhur DY, Shafaei J, Derakhshan H, Ingham JM. In situ out-of-plane testing of unreinforced masonry cavity walls in as-built and improved conditions. Structures 2015;3:187–99. https://doi.org/10.1016/j.istruc.2015.04.005.
[34] Sena-Cruz J, Barros J, Bianco V, Bilotta A, Bournas D, Ceroni F, et al. NSM systems. RILEM State-of-the-Art Rep 2016;19:303–48. https://doi.org/10.1007/978-94-017-7336-2_8.
[35] Pasca M, Liberatore L, Masiani R. Reliability of analytical models for the prediction of out-of-plane capacity of masonry infills. Struct Eng Mech 2017;64:765–81. https://doi.org/10.12989/sem.2017.64.6.765.
[36] Angel R, Abrams D, Shapiro D, Uzarski J, Webster M. Behavior of reinforced concrete frames with masonry infills, University of Illinois Engineering Experiment Station. College of Engineering. University of Illinois at Urbana-Champaign. ISSN: 0069-4274. vol. SRS-589; 1994.
[37] Abrams DP, Angel R, UJ. Out of plane strength of unreinforced masonry infill panels. Earthq Spectra 1996;12:825–44.
[38] Eurocode 6. Design of Structures for Earthquake Resistance, Part 1: General rules, seismic actions and rules for buildings Masonry Structures, European Committee for Standardization; Brussels, Belgium; 2005.
[39] Ricci P, Di Domenico M, Verderame GM. Experimental assessment of the in-plane/out-of-plane interaction in unreinforced masonry infill walls. Eng Struct 2018. https://doi.org/10.1016/j.engstruct.2018.07.033.
[40] Bashandy T, Rubiano NR, Klingner RE. Evaluation and analytical verification of infilled frame test data; 1995.
[41] FEMA 306. Evaluation of earthquake damaged concrete and masonry wall buildings - Basic Procedures Manual, prepared by ATC Applied Technology Council, Federal Emergency Management Agency, Washington D.C.,USA; 1998.
[42] NZSEE. New Zealand Society for Earthquake Engineering. The Seismic Assessment of Existing Buildings. Technical Guidelines for Engineering Assessments. Part C: Moment Resisting Frames with Infill Panels; 2017.
[43] Tomassetti U, Graziotti F, Penna A, Magenes G. Modelling one-way out-of-plane response of single-leaf and cavity walls. Eng Struct 2018;167:241–55. https://doi.org/10.1016/j.engstruct.2018.04.007.
[44] Graziotti F, Tomassetti U, Sharma S, Grottoli L, Magenes G. Experimental response of URM single leaf and cavity walls in out-of-plane two-way bending generated by seismic excitation. Constr Build Mater 2019;195:650–70. https://doi.org/10.1016/j.conbuildmat.2018.10.076.
[45] Singhal V, Rai DC. Role of toothing on in-plane and out-of-plane behavior of confined masonry walls. J Struct Eng (United States) 2014;140:1–14. https://doi.org/10.1061/(ASCE)ST.1943-541X.0000947.
[46] Griffith MC, Vaculik J, Lam NTK, Wilson J, Lumantarna E. Cyclic testing of unreinforced masonry walls in two-way bending. Earthq Eng Struct Dyn 2007;36:801–21. https://doi.org/10.1002/eqe.654.
[47] Akhoundi F, Vasconcelos G, Lourenço PB, Silva LM. Out-of-plane response of masonry infilled RC frames: effect of workmanship and opening. 16th Int. Brick Block Mason. Conf. 2016:1147–54.
[48] Wang C. Experimental Investigation on the Out-Of-Plane behaviour of concrete masonry infilled frame. Nova Scotia: Dalhousie University Halifax; 2017.
[49] Sepasdar R. Experimental investigation on the out-of-plane behaviour of concrete masonry infilled RC frames. Nova Scotia: Dalhousie University Halifax; 2017.
[50] Kinstlinger J. Behavior of wall panels under static and dynamic loads. Massachusetts Institute of Technology; 1952.
[51] Frederiksen VT. Membrane effect in laterally loaded masonry walls. A second order phenomenon. In: 6th Can Mason Symp, Saskatoon, Saskatchewan; 1992. p. 537–47.
[52] Flanagan RD. Behavior of structural clay tile infilled frames. Knoxville: University of Tennessee; 1994.
[53] Flanagan R, Bennett R. Bidirectional behavior of structural clay tile infilled frames. J Struct Eng 1999;125:236–44. https://doi.org/10.1061/(ASCE)0733-9445(1999)125:3(236).
[54] Beconcini ML. Sulla resistenza a forze orizzontali di pareti in elementi forati di laterizio. Costr Laterizio 1997;55:60–9.
[55] Calvi GM, Bolognini D. Seismic response of reinforced concrete frames infilled with weakly reinforced masonry panels. J Earthq Eng 2001;5:153–85. https://doi.org/10.1080/13632460109350390.
[56] Modena C, da Porto F. Ricerca sperimentale sul comportamento fuori piano di tamponamenti in muratura in zona sismica. Padova, Italy; 2005.
[57] Komaraneni S, Rai DC, Singhal V. Seismic behavior of framed masonry panels with prior damage when subjected to out-of-plane loading. Earthq Spectra 2011;27:1077–103. https://doi.org/10.1193/1.3651624.
[58] Varela-Rivera JL, Navarrete-Macias D, Fernandez-Baqueiro LE, Moreno EI. Out-of-plane behaviour of confined masonry walls. Eng Struct 2011;33:1734–41. https://doi.org/10.1016/j.engstruct.2011.02.012.
[59] Varela-Rivera J, Moreno-Herrera J, Lopez-Gutierrez I, Fernandez-Baqueiro L. Out of plane strength of confined masonry walls. J Struct Eng 2012;138:1331–41. https://doi.org/10.1061/(ASCE)ST.1943-541X.0000578.
[60] Pereira MFP, Pereira MFN, Ferreira JED, Lourenço PB. Behavior of masonry infill panels in RC frames subjected to in plane and out of plane loads. In: Amcm2011 - 7th Int Conf Anal Model New Concepts Concr Mason Struct; 2011.
[61] Pereira MFP, Pereira MFN, Ferreira JE, Lourenço PB. Infill masonry: simple analytical methods for seismic design. In: 9th Int Mason Conf; 2014. p. 1–12.
[62] da Porto F, Guidi G, Dalla Benetta M, Verlato N. Combined in-plane/out-of-plane experimental behaviour of reinforced and strengthened infill masonry walls. In: 12th Can Mason Symp; 2013. p. 1–11.
[63] Dizhur D, Walsh K, Giongo I, Derakhshan H, Ingham J. Out-of-plane proof testing of masonry infill walls. Structures 2018;15:244–58. https://doi.org/10.1016/j.istruc.2018.07.003.
[64] Walsh K, Dizhur D, Giongo I, Derakhshan H, Ingham J. Predicted versus experimental out-of-plane force-displacement behaviour of unreinforced masonry walls. Structures 2018;15:292–306. https://doi.org/10.1016/j.istruc.2018.07.012.
[65] Hak S, Morandi P, Magenes G. Out-of-plane experimental response of strong masonry infills. In: Second Eur Conf Earthq Eng Seismol., Istanbul; 2014. p. 1–12.
[66] Furtado A, Rodrigues H, Arêde A, Varum H. Experimental evaluation of out-of-plane capacity of masonry infill walls. Eng Struct 2016;111:48–63. https://doi.org/10.1016/j.engstruct.2015.12.013.
[67] De Risi MT, Di Domenico M, Ricci P, Verderame GM, Manfredi G. Experimental investigation on the influence of the aspect ratio on the in-plane/out-of-plane interaction for masonry infills in RC frames. Eng Struct 2019;189:523–40. https://doi.org/10.1016/j.engstruct.2019.03.111.
[68] Di Domenico M, Ricci P, Verderame GM. Experimental assessment of the out-of-plane strength of URM infill walls with different slenderness and boundary conditions. Bull Earthq Eng 2019. https://doi.org/10.1007/s10518-019-00604-5.
[69] Morandi P, Hak S, Magenes G. Simplified Out-of-plane Resistance Verification for Slender Clay Masonry Infills in RC Frames. In: Proc 15th Natl Ital. Conf Seism Eng, Padua; 2013.
[70] Zizzo M, Cavaleri L, Di Trapani F. Out of plane capacity of infills after in plane loading: a prediction analitical model. In: COMPDYN 2019, 7th ECCOMAS Themat conf comput methods struct dyn earthq eng, Crete, Greece, 24–26 June; 2019.
[71] Liberatore L, Decanini LL. Seismic lateral deformation and energy demands in bare and infilled RC frames. In: 13th World Conf Earthq Eng; 2004. p. 1–13.
[72] LSTC Livermore Software Technology Corporation. LS_DYNA Keyword User's Manual; 2013.
[73] Liberatore L, Bruno M, Al Shawa O, Pasca M, Sorrentino L. Finite-discrete element modelling of masonry infill walls subjected to out-of-plane loads. In: ECCOMAS Congr 2016 - Proc 7th Eur Congr Comput Methods Appl Sci Eng, vol. 3; 2016. doi:10.7712/100016.2175.8924.
[74] Hallquist J. LS-DYNA® Theory Manual. LS-DYNA Theory Man.; 2006.
[75] Burnett S, Gilbert M, Molyneaux T, Beattie G, Hobbs B. The performance of unreinforced masonry walls subjected to low-velocity impacts: finite element analysis. Int J Impact Eng 2007;34:1433–50. https://doi.org/10.1016/j.ijimpeng.2006.08.004.
[76] AlShawa O, Sorrentino L, Liberatore D. Simulation of shake table tests on out-of-plane masonry buildings. Part (II): combined finite-discrete elements. Int J Archit Herit 2017. https://doi.org/10.1080/15583058.2016.1237588.
[77] Broadhouse B, Neilson A. Modelling reinforced concrete structures in DYNA3D. Report: AEEW-M 2465. Safety and Engineering Science Division, United Kingdom Atomic Energy Authority. Winfrith Technology Center. Dorchester, UK; 1987.
[78] Drysdale RG, Essawy AS. Out-of-plane bending of concrete block walls. J Struct Eng 1988;114:121–33.
[79] Anić F, Penava D, Abrahamczyk L, Sarhosis V. Computational evaluation of experimental methodologies of out-of-plane behavior of framed-walls with openings. Earthq Struct 2019;16:265–77. https://doi.org/10.12989/eas.2019.16.3.265.
[80] Griffith M, Vaculik J. Out-of-plane flexural strength of unreinforced clay brick masonry walls. Mason Soc J 2007:53–68.
[81] Vaculik J, Griffith M. Out-of-plane load–displacement model for two-way spanning masonry walls. Eng Struct 2017;141:328–43. https://doi.org/10.1016/j.engstruct.2017.03.024.